CHARACTERIZATION UF UNCONVENTIONAL RESERVOIRS USING MULTIPHASE FLOW AND SEISMIC WAVE PROPAGATION SIMULATORS

Naddia Arenas[a,b], Gabriela Savioli[a], Patricia Gauzellino[b] and Juan Santos[a,c]

[a]*Departamento de Energía, Instituto del Gas y del Petróleo, , Universidad de Buenos Aires, Av. Las Heras 2214 Piso 3 C1127AAR Buenos Aires, Argentina, ingnaddiarenas@gmail.com, gsavioli@fi.uba.ar*

[b]*Facultad de Ciencias Astronómicas y Geofísicas, Universidad Nacional de La Plata, Paseo del Bosque s/n, B1900FWA, La Plata, Argentina, gauze@fcaglp.unlp.edu.ar*

[a,c]*Department of Mathematics, Purdue University, 150 N. University Street, West Lafayette, Indiana, 47907-2067, USA, jesantos48@gmail.com*

Keywords: Modeling, multiphase flow, seismic waves, uncoventional reservoirs.

Abstract. The aim of this work is the study and characterization of shale gas reservoirs using numerical simulators of multiphase flow and seismic wave propagation in porous media. In these unconventional reservoirs the hydrocarbons production is carried out by hydraulic fracturing through the injection of fluids at high pressures. The effect of injection is a pore pressure increase, and, consequently, the zones of greater weakness are fractured, incrementing permeability and porosity values in the stimulated region. Thus, the modeling of fluid flow and the identification and characterization of fractures through seismic analysis are very important in these environments. A public domain Black-Oil simulator (BOAST) is applied to model the fluid injection process into the reservoir during hydraulic fracturing. This is combined with a fracture criterion based on a breakdown pressure and a subsequent updating of rock properties in the fractured zone. The fractures can be detected by applying a wave propagation simulator based on a poroviscoelastic model that includes attenuation and dispersion effects due to rock heterogeneities and the presence of fluids. The results show the ability of the described techniques to model the generation of fractures and, subsequently, to detect their presence.

1 INTRODUCTION

In low or ultra-low permeability reservoirs hydraulic fracturing is essencial to allow hydrocarbon production. This treatment begins by pumping a fluid inside the wellbore which causes a rise in pore pressure and leads to the initiation of the fracture. In this way, new fractures are created that joint with existing natural fractures create a path by which the hydrocarbons flow towards the wellbore (Riahi and Damjanac, 2013). Different models have been developed to represent this process, but they are either too simplified or they only consider a few aspects of fracking (Zhao et al., 2014). Besides it is common to disregard the influence of the fluid (Hattori et al., 2017) A detailed description of hydraulic fracturing models can be seen in (Adachi et al., 2007).

In this work fracture propagation is represented combining water injection with a rock rupture criterion, based on a breakdown pressure.The procedure is carry out in sequential steps. In each step the fluid injection is modeled applying a Black-Oil simulator Aziz and Settari (1985) and the final pore pressure is analyzed: if it becomes greater than the breakdown pressure in a grid block, that block is fractured increasing permeability and porosity values. Finally, with the updated properties and using final pressures and saturations of the actual step as initial values of the following, a new step starts (Savioli et al., 2018). The Black-Oil simulator is the public domain software BOAST (Fanchi, 1997) and the breakdown pressure follows the weakness zones determined by the stress distribution map. In fact the influence of weakness zones in fracture propagation is analyzed in this work while the effect of natural fractures was studied in (Savioli et al., 2018).

Once the fracture is complete, a seismic monitoring procedure is applied to identify its location. The presence of the injected water and the increment in rock properties affect seismic response (Sena et al., 2011). It is well known that mesoscopic losses are the main attenuation mechanism in fluid saturated porous media (Muller et al., 2010).They are caused by heterogeneities in the fluid and solid phase properties greater than the pore size but much smaller than the predominant wavelengths Therefore, a wave propagation simulator, based on an isotropic viscoelastic model that considers dispersion and attenuation effects, is applied (Picotti et al., 2010; Savioli et al., 2017)

2 THEORY

2.1 Black-Oil formulation for Gas-Water flow in porous media

The diferential equations of the Black-Oil model applied to two-phase (gas phase, subindex g, and aqueous phase, subindex w) and two component (Gas and Water) fluid flow are (Savioli et al., 2018),

$$\nabla \cdot (\underline{\kappa}(\frac{\kappa_{rg}}{B_g \eta_g}(\nabla p_g - \rho_g g \nabla D) + \frac{R_s \kappa_{rw}}{B_w \eta_w}(\nabla p_w - \rho_w g \nabla D))) + \frac{q_g}{\rho_g^{SC}} = \frac{\partial \left[\phi \left(\frac{S_g}{B_g} + \frac{R_s S_w}{B_w}\right)\right]}{\partial t}, \tag{1}$$

$$\nabla \cdot (\underline{\kappa}\frac{\kappa_{rw}}{B_w \eta_w}(\nabla p_w - \rho_w g \nabla D)) + \frac{q_w}{\rho_w^{SC}} = \frac{\partial \left[\phi \frac{S_w}{B_w}\right]}{\partial t}. \tag{2}$$

where the unknowns are the phase pressures, p_g, p_w, and the phase saturations S_g, S_w. In eqs (1)- (2), ϕ is porosity, $\underline{\kappa}$ is the absolute permeability tensor, assumed to be diagonal $\underline{\kappa} = \text{diag}(\kappa_x, \kappa_y, \kappa_z)$, D indicates depth, and g is the gravity constant. For $\beta = g, w$, ρ_{beta}, ρ_{beta}^{SC} are densities at reservoir and standard conditions, respectively; functions $k_{r\beta}$ and η_β are the relative permeability and viscosity of the β-phase, respectively. Besides, the Black-Oil model considers a simplified thermodynamic model, represented by the PVT data: R_s (Gas solubility in aqueous phase), B_g (Gas formation volume factor) and B_w ($Water$ formation volume factor).

Two algebraic equations complete the system

$$S_w + S_g = 1, \qquad p_g - p_w = P_C(S_w), \tag{3}$$

where P_C is the capillary pressure.

The solution of the Black-Oil model is obtained applying the public domain software BOAST (Fanchi, 1997) which solves the differential equations using the IMPES (IMplicit Pressure Explicit Saturation) finite difference technique. The details can be seen in (Savioli et al., 2018).

2.2 Fracture Criterion

To fracture the porous media, water is injected at high pressure. The injection produces an increase in pore pressure ($p = S_g p_g + S_w p_w$) and, consequently, the rock breaks following its areas of weakness. The method neeeds a $breakdown\,pressure$ (P_{bd}) distribution as an input data. During the injection, once pore pressure becomes greater than the breakdown pressure on a certain cell, this cell is fractured, .ie., permeability and porosity are incremented in the weakness area.

The $breakdown\,pressure$ can be computed from the horizontal stress σ_H and the tensile stress of the rock T_0 (Economides and Hill, 1994) as follows,

$$P_{bd} = 3\sigma_{Hmin} - \sigma_{Hmax} + T_0 - p_H, \tag{4}$$

where

$$\sigma_{Hmax} = \sigma_{Hmin} + \sigma_{Tect} \tag{5}$$

being σ_{Tect} the tectonic stress contribution and σ_{Hmin} the minimum horizontal stress obtained from the vertical stress σ_v.

2.3 Seismic Modeling: A viscoelastic model for wave propagation

The propagation of waves in porous media is described using a viscoelastic model that takes into account the dispersion and attenuation effects due to the presence of heterogeneities in the fluid and solid phases properties.

The equation of motion in a 2D isotropic viscoelastic domain Ω with boundary $\partial\Omega$ is (Santos et al., 2011):

$$\omega^2 \rho u + \nabla \cdot \sigma(u) = f(x, \omega), \quad \Omega, \tag{6}$$

with boundary condition:

$$-\sigma(u)\nu = i\omega \mathcal{D} u, \quad \partial\Omega. \tag{7}$$

where $u = (u_x, u_z)$ is the displacement vector, $\rho = (1 - \phi)\rho_s + \phi\rho_f$ is the bulk density, $f(x, \omega)$ is the external source and (7) is a first-order absorbing boundary condition using the

positive definite matrix $\mathcal{D}$ (Ha et al., 2002). Note that this viscoelastic model considers single phase fluid, so the fluid density ρ_f is obtained weighting the gas and water densities with their respective saturations, i.e. $\rho_f = \rho_g S_g + \rho_w S_w$.

The numerical solution is computed at a selected number of frequencies in the range of interest using an iterative finite element domain decomposition procedure. The time domain solution is obtained using a discrete inverse Fourier transform (Ha et al., 2002) . To approximate each component of the solid displacement vector we employ a nonconforming finite element space which generates less numerical dispersion than the standard bilinear elements.

3 NUMERICAL RESULTS

We model a shale reservoir volume of 7.3 m $\times$ 44 m $\times$ 44 m with a mesh of 60 $\times$ 120 $\times$ 120 cells. The mesh is refined around the injection point, located in block (30, 60, 90) i.e., there is a 30 $\times$ 60 $\times$ 60 inner zone with $\Delta x = 0.2ft = 0.06096\,m$, $\Delta y = \Delta z = 0.4ft = 0.12192\,m$ and a 30 $\times$ 60 $\times$ 60 outer zone with $\Delta x = \Delta y = \Delta z = 2ft = 0.6096\,m$.

The matrix permeability and porosity are considered constant, $\kappa_m = 0.0001$ mD and $\phi_m = 0.1$, respectively. When the rock is fractured these properties increase and take new values, $\kappa_f = 10000$ mD and $\phi_f = 0.5$. We apply the hypothesis that the fracture propagates in the (y-z) plane and use the breakdown pressure distribution of Figure 1 as an input data. Figure 1 represents the reservoir weakness areas that will determine the progress of the fracking process.

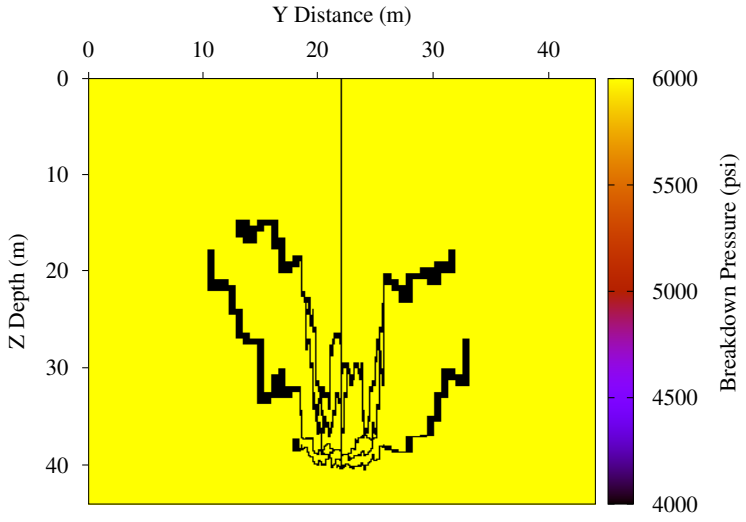

Figure 1: Weakness area distribution in the 2D section

The injection process begins with an initial flow rate of 0.088 m^3/s which is increased every 40 minutes until reaching 0.52 m^3/s. Figure 2 shows the evolution of pressure distribution in the (y-z) fracture plane as injection time increases. At early times, we can observe that pressure grows around the injection point following the weakness zone shape. This increment causes the rock rupture represented by a permeability magnification in the affected cells, consequently the injected water enters in the fracture zone, as Figure 3 shows. Figures 2 and 3 illustrate the fracture evolution and the displacement of the injected water: initially water saturation distribution also follows the weakness zone shape but later, as flow increases, water invades a greater area.

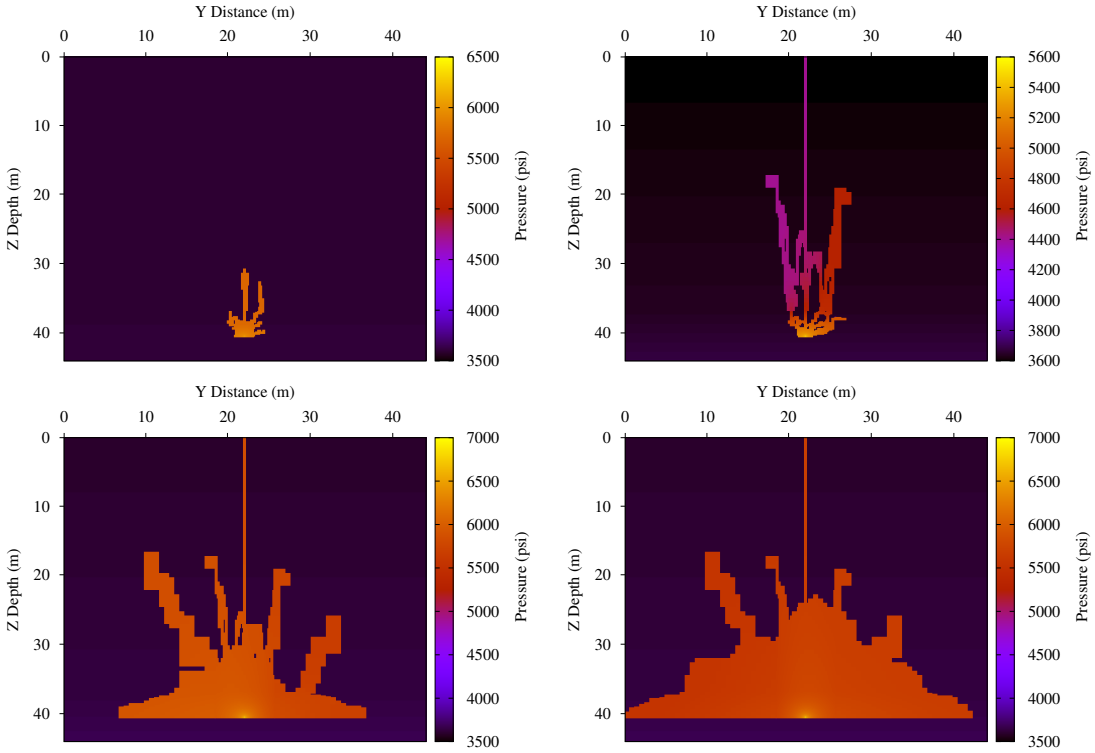

Figure 2: Pressure distribution in the 2D section after 9 seconds, 10 minutes, 1 hour and 1 hour and 40 minutes of injection

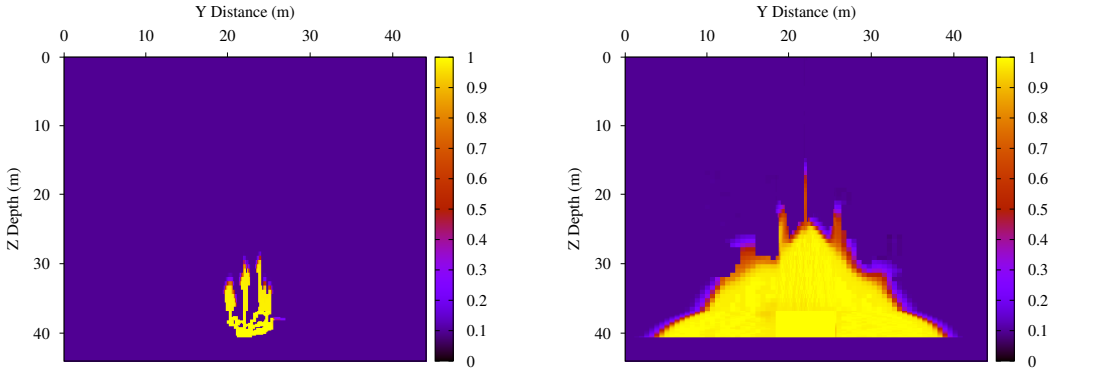

Figure 3: Saturation distribution in the 2D section after 10 minutes and 1 hour and 40 minutes of injection

Figure 4 shows the times in which the cells are fractured in a color scale. Time increases from cold colors (early stages) to warm colors (late stages). Again, from this figure it is evident that in the early stages the fracture follows the shape of the weakness area but then tends to spread occupying the entire plane. In addition this advance occurs concentrically at the same time.

To identify and characterize the fracture, seismic monitoring of the reservoir is performed. The point source is placed 150 m from the injection point and a line of vertical receivers is also placed at 150 m but on the opposite side.

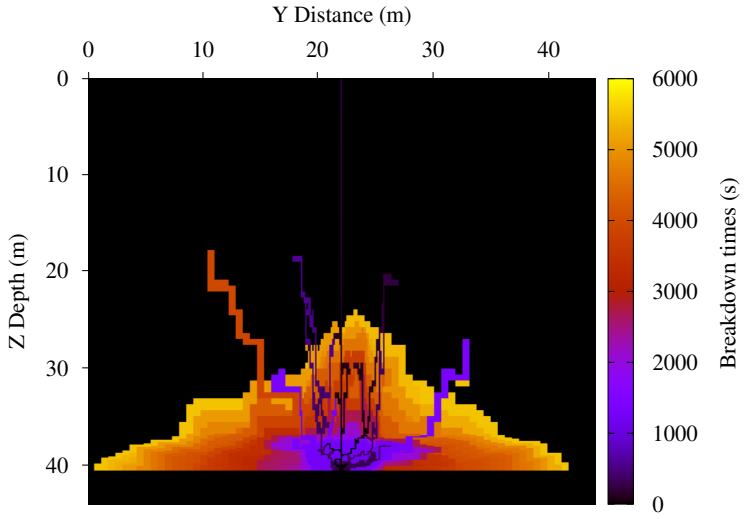

Figure 4: Breakdown times during the fracking process

Figure 5 illustrates the z-component behavior of vertical velocity at 105 ms and 120 ms. The 105 ms snapshot shows the incident P-wave arriving to the fracture and also a S-wave traveling behind it. At 120 ms we can observe the reflected P-wave travelling to the left: this reflection is generated by the presence of water in the fracture. Again, the other wavefront is the S-wave generated by the point source. This fact is verified in Figure 6 that compares the z-component of vertical velocity at 140 ms before (left) and after (right) applying the divergence operator, which removes the S-wave.

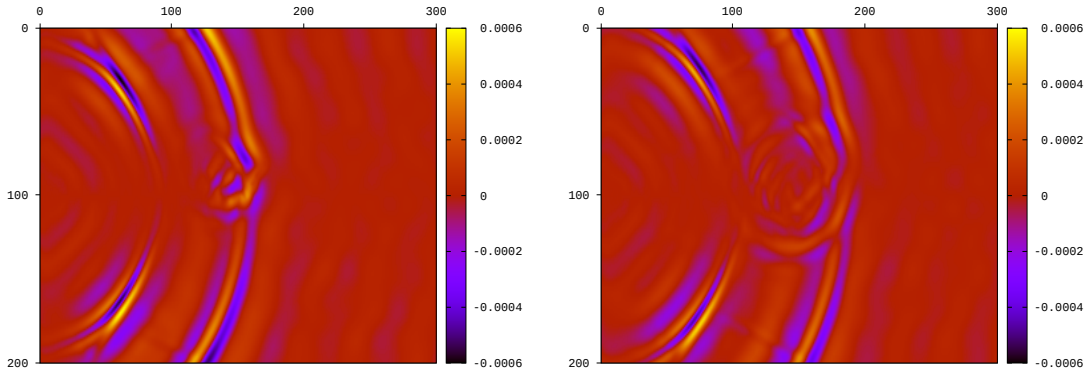

Figure 5: Snapshots of z-component of velocity at 105 ms and 120 ms.

4 CONCLUSIONS

This work models a fracking procedure in shale gas reservoirs, as well as fracture characterization through seismic monitoring. The applied methodology consists of using a multiphase fluid simulator combined with a fracture criterion together with a wave propagation simulator based on a viscoelastic model. The fluid injection increases reservoir pressure and this increment causes rock rupture in weakness zones From the numerical results we conclude that:

- The fracture evolution begins following the weakness zone shape and later it spreads out

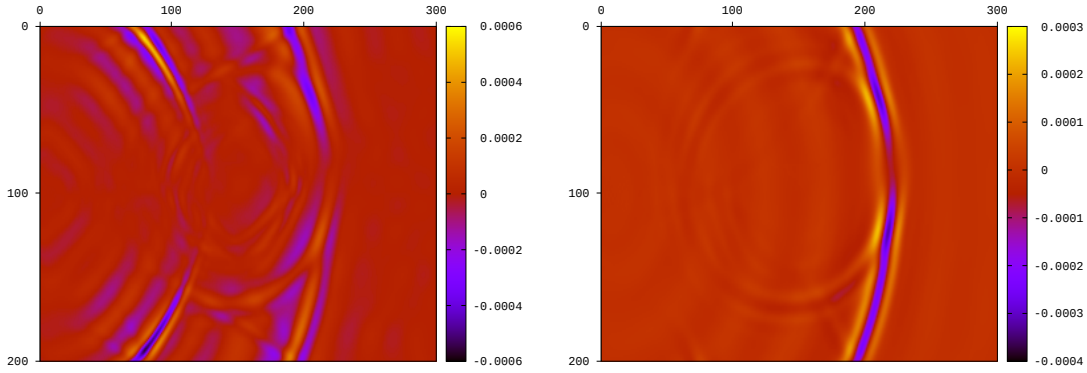

Figure 6: Snapshots of vertical velocity (left) and velocity divergence (right) at 140 ms.

occupying the entire plane. Besides the advance occurs concentrically at the same time This behavior is in agreement with actual microseismic data that exhibit planar and bi-wing fractures.

- During the fracking process the injected water invades the porous medium due to permeability increment but water front advance is delayed compared with the fractured zone.
- The application of poroviscoelastic wave propagation simulator shows that seismic monitoring is able to identify the presence of the stimulated area due to hydraulic fracturing.

ACKNOWLEDGEMENTS

This work was partially funded by ANPCyT, Argentina (PICT 2015 1909) and Universidad de Buenos Aires (UBACyT 20020160100088BA).

REFERENCES

Adachi J., Siebrits E., Peirce A., and Desroches J. Computer simulation of hydraulic fractures. *International Journal of Rock Mechanics and Mining Sciences*, 44:739–757, 2007.

Aziz K. and Settari A. *Petroleum Reservoir Simulation*. Elsevier Applied Science Publishers, Great Britain, 1985.

Economides M.J. and Hill A.D. *Petroleum Production Systems*. Prentice Hall PTR, New Jersey, USA, 1994.

Fanchi J. *Principles of Applied Reservoir Simulation*. Gulf Professional Publishing Company, Houston, Texas, 1997.

Ha T., Santos J., and Sheen D. Nonconforming finite element methods for the simulation of waves in viscoelastic solids. *Comput. Meth. Appl. Mech. Engrg.*, 191:5647–5670, 2002.

Hattori G., Trevelyan J., Augarde C.E., Coombs W.M., and Aplin A.C. Numerical simulation of fracking in shale rocks: Current state and future approaches. *Archives of Computational Methods in Engineering*, 24:281–317, 2017.

Muller T., Gurevich B., and Lebedev M. Seismic wave attenuation and dispersion resulting from wave-induced flow in porous rocks. *Geophysics*, pages A147–A164, 2010.

Picotti S., Carcione J., Rubino G., Santos J., and Cavallini F. A viscoelastic representation of wave attenuation in porous media. *Comput. Geosci*, 36:44–53, 2010.

Riahi A. and Damjanac B. Numerical study of interaction between hydraulic fracture and discrete fracture network. In A. Bunger, J. McLennan, and R. Jeffrey, editors, *Effective and Sustainable Hydraulic Fracturing*. INTECH, 2013.

Santos J.E., Carcione J.M., and Picotti S. Analysis of mesoscopic loss effects in anisotropic poroelastic media using harmonic finite element simulations. *Proc. 81th Annual International Meeting SEG (San Antonio)*, pages 2211–2215, 2011.

Savioli G., Santos J., Gauzellino P., and Lavia M. Modeling multiphase fluid flow in unconventional reservoirs. *Mecanica Computacional*, 36:1263–1275, 2018.

Savioli G., Santos J.E., Carcione J.M., and Gei D. A model for co2 storage and seismic monitoring combining multiphase fluid flow and wave propagation simulators. the sleipner-field case. *Computational Geosciences*, 21:223–239, 2017.

Sena A., Castillo G., Chesser K., Voisey S., Estrada J., Carcuz J., Carmona E., and Hodgkins P. Seismic reservoir characterization in resource shale plays: Stress analysis and sweet spot discrimination. *The Leading Edge*, pages 758–764, 2011.

Zhao J., Li Y., Wang S., Jiang Y., and Zhang L. Simulation of complex fracture networks influenced by natural fractures in shale gas reservoir. *Natural Gas Industry B*, pages 89–95, 2014.